Available online at www.sciencedirect.com
ScienceDirect
Journal of the European Ceramic Society 29 (2009) 3205–3209
www.elsevier.com/locate/jeurceramsoc

High-temperature mechanical behavior of Al_2O_3/graphite composites

Eugenio Zapata-Solvas [a], Rosalía Poyato [a], Diego Gómez-García [a], Arturo Domínguez-Rodríguez [a,*], Nitin P. Padture [b]

[a] *Departamento Física de la Materia Condensada, Universidad de Sevilla, 41080 Sevilla, Spain*
[b] *Department of Materials Science & Engineering, Center for Emergent Materials, The Ohio State University, Columbus, OH 43210, USA*

Received 31 March 2009; received in revised form 28 May 2009; accepted 4 June 2009
Available online 7 July 2009

Abstract

Uniaxial compressive creep behaviour of spark-plasma-sintered Al_2O_3/graphite particulate composites has been studied at temperature between 1250 and 1350 °C. Values of stress exponent, n, ranging from 1 to 1.4 and, activation energy, Q, of 600 ± 40 kJ/mol have been determined. With 10 vol% graphite in the composite, the creep deformation of the composite is controlled by the fine-grained Al_2O_3 matrix, where Coble creep has been identified as the dominant creep mechanism.

Keywords: Composites; Ceramics; Graphite; Creep

1. Introduction

There have been extensive studies on the high-temperature deformation of pure Al_2O_3 polycrystalline ceramics.[1–3] Research in high-temperature deformation of Al_2O_3 is driven by opposing goals, while suppressing cavitation in both cases[3]: (i) decrease creep resistance for improved superplastic forming and (ii) increase creep resistance for improved high-temperature mechanical properties.

There have been efforts to increase steady-state creep rate in Al_2O_3 by suppressing grain growth, through MgO doping[4] or TiO_2/MgO codoping[5] or CuO/MgO codoping.[6] However, ductility-limiting concurrent grain growth was still found to occur. Grain-boundary pinning by second-phase particle dispersion has been found to be more effective in suppressing grain growth, resulting in improved ductility of Al_2O_3 with dispersions of $Mg_2Al_2O_4$,[7] ZrO_2,[8] and combined $Mg_2Al_2O_4$/ZrO_2.[9]

In contrast, significant decreases in steady-state creep rates, between 1 and 2 orders of magnitude, have been reported in Al_2O_3 singly doped with Zr, Y, La, or Nd[10] and codoped with Nd/Zr.[11,12] The origin of grain growth suppression and creep resistance enhancement appears to be related with the decrease of grain-boundary diffusivity.[13] However, we did not observe C in the HRTEM we performed. In any case it is difficult to ascribe the same behaviour to C, than Zr, Y, Nb, Ca, *etc*. because the radius of C is much smaller. For instance, in Y_2O_3-stabilised tetragonal ZrO_2 polycrystals (YTZP) it has been shown that cations with smaller ionic sizes decrease the flow stress, whereas those with larger ionic sizes increase the flow stress.[14,15]

More recently Al_2O_3 ceramics (0.5 μm grain size) containing a 10 vol% dispersion of single-wall carbon nanotubes (SWNTs) fabricated using spark-plasma sintering (SPS)[16,17] has been found to be about 2 orders of magnitude more creep-resistant compared to pure Al_2O_3 of the same grain size.[18,19] The high-temperature deformation mechanisms in these Al_2O_3/SWNTs composites are intimately related to their unique grain-boundary structures,[20,21] where high-temperature stretching of SWNTs appears to impede grain-boundary sliding.[18]

In a related study, nanocomposites of Al_2O_3 with a dispersion of 10 vol% graphite particles were also fabricated using the SPS method.[16] These Al_2O_3/graphite composites were found to be resistant to contact damage under indentation.[16] The objective of this research is to study and model the high-temperature deformation of these interesting composites.

2. Experimental

The Al_2O_3/graphite particulate composites with 10 vol% graphite used here are from a previous study.[16] The fabricated

* Corresponding author. Tel.: +34 954 557849.
E-mail address: adorod@us.es (A. Domínguez-Rodríguez).

0955-2219/$ – see front matter © 2009 Elsevier Ltd. All rights reserved.
doi:10.1016/j.jeurceramsoc.2009.06.002

procedure is reported in 16, and is summarized here. A mixture of Al_2O_3 nanopowders and graphite particles (~2 μm size) were dispersed in methanol with the aid of ultrasonic agitation. The dried powder blend was then spark-plasma sintered (SPS) at 1450 °C with a five minutes holding time. The density of the as-fabricated Al_2O_3/graphite composites is 3.713 Mg m^{-3}, which is 97.7% of the theoretical limit.[16]

The Al_2O_3/graphite composites were cut into 4 mm × 2 mm × 2 mm rectangular parallelepipeds samples for creep testing. Uniaxial-compression creep testing was performed using the method and equipment described elsewhere.[22] The applied stresses (σ) were in the ranges 166–350, 53–190 and 20–80 MPa at temperatures (T) 1250, 1300 and 1350 °C, respectively. The temperatures used are high enough for detectable diffusion processes to occur. Argon gas atmosphere was used to prevent oxidation of the graphite particles.

Slices from the Al_2O_3/graphite composites were prepared using conventional TEM-specimen-preparation methods, involving successive steps of grinding, polishing, dimpling, and ion-beam milling. Liquid nitrogen cooling was used in the latter to minimize ion-beam damage (Fischione Instruments, Export, PA). Scanning electron microscopy (SEM) samples from the Al_2O_3/graphite composites were prepared using conventional methods. Microstructures of the Al_2O_3/graphite composites, before and after creep testing, were investigated using transmission electron microscopy (TEM). A conventional TEM (CM-200, Philips Electron Optics, Eindhoven, The Netherlands) operated at 200 kV and a high resolution TEM (HRTEM) operated at 300 kV (CM-300, Philips Electron Optics, Eindhoven, The Netherlands) at the National Center for Electron Microscopy, Lawrence Berkeley National Laboratory, California, USA were used. Carbon elemental analysis was acquired by energy dispersive spectrometer (EDS), attached to the CM-200 TEM, to delineate the graphite-particles distribution. A conventional SEM (JSM 5400, JEOL, Tokyo, Japan) operated at 20 kV at the Instituto de Ciencias de Materiales de Sevilla, Universidad de Sevilla, C.S.I.C. (Spain).

Grain size measurements were performed on the TEM images using standard procedures; at least 300 Al_2O_3 grains were used for the measurement.

3. Results

Fig. 1a is an electron back-scattering SEM micrograph at low magnification and Fig. 1b is a bright-field (BF) TEM image of the as-received Al_2O_3/graphite composite. Note the fine-grained equiaxed nature of the ploycrystalline Al_2O_3 matrix and the non-equiaxed nature of the graphite particles. The average size of the Al_2O_3 grains is found to be 0.95 ± 0.07 μm. Inset in Fig. 1 is a selected area electron diffraction pattern, confirming the graphite phase. The local chemical analysis in Fig. 2 further confirms the presence of the graphite phase. Fig. 2a shows a BF TEM image, and Fig. 2b shows corresponding EDS data across the line in Fig. 2a.

Fig. 3 is a typical creep curve at 1250 °C showing different values of the stress exponent n. The steady-state creep data for the Al_2O_3/graphite composite, in the form of steady-state strain

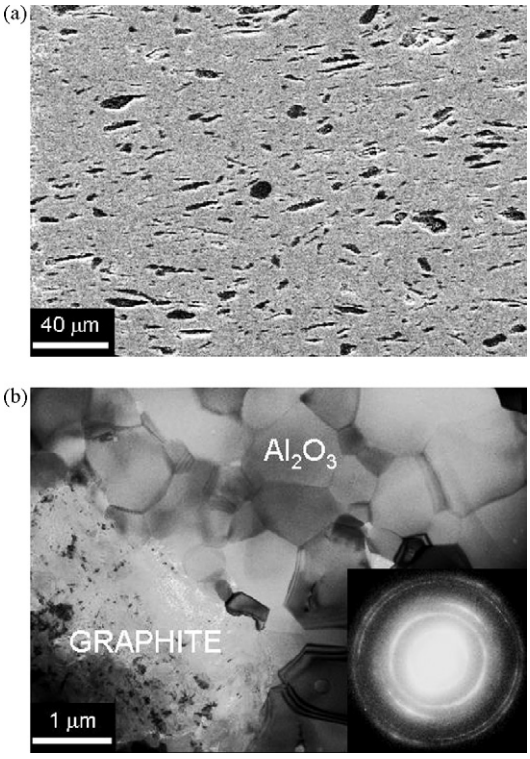

Fig. 1. Micrographs of the Al_2O_3/graphite composite. (a) Electron back-scattering SEM at low magnification (graphite are identified as black particles) and (b) bright-field TEM at high magnification. Inset (b) is a SAEDP from the graphite inclusion.

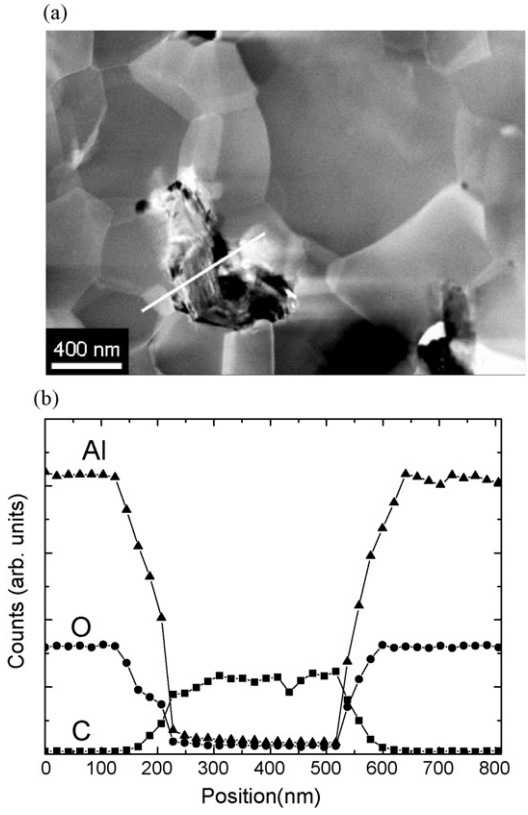

Fig. 2. (a) Bright-field TEM micrograph of the Al_2O_3/graphite composite, and (b) corresponding EDS chemical analysis (normalized counts) along the dotted line denoted in (a).

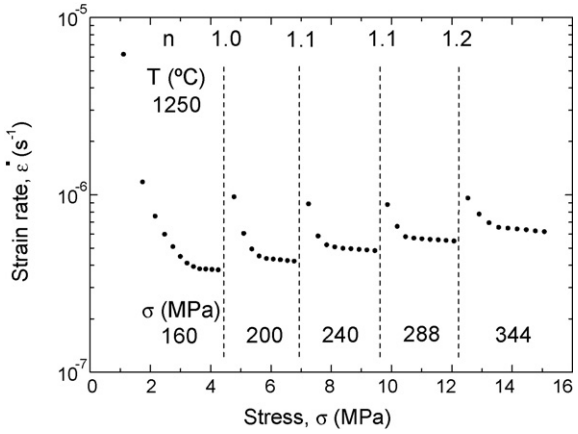

Fig. 3. Typical creep curve of Al_2O_3/graphite composite deformed at 1250 °C. It is shown also change of stress to determine the stress exponent.

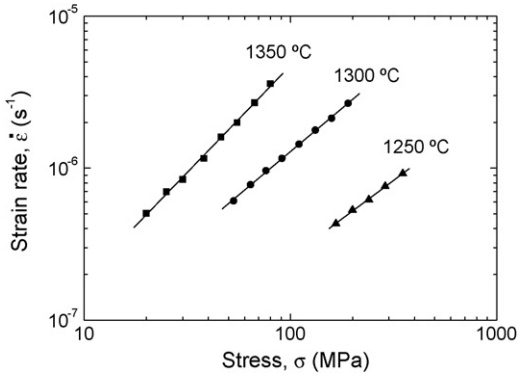

Fig. 4. Steady-state creep data for Al_2O_3/graphite composite at 1250, 1300, and 1350 °C. The straight lines are best fits to the data.

rate, $\dot{\varepsilon}$, versus σ, are plotted in Fig. 4. These data in the plots are for tests at 1250, 1300 and 1350 °C, and the straight lines are linear fits. Fig. 5 shows the $\dot{\varepsilon}$ versus σ data at 1350 °C for pure Al_2O_3 and Al_2O_3/10 vol% SWNTs composite from the literature, and the Al_2O_3/graphite composite. It can be seen that pure Al_2O_3 is less creep resistant[23] compared with Al_2O_3/SWNTs[18,19] and Al_2O_3/graphite composites. On the other hand, different slopes for Al_2O_3/SWNT and Al_2O_3/graphite composites are a clear

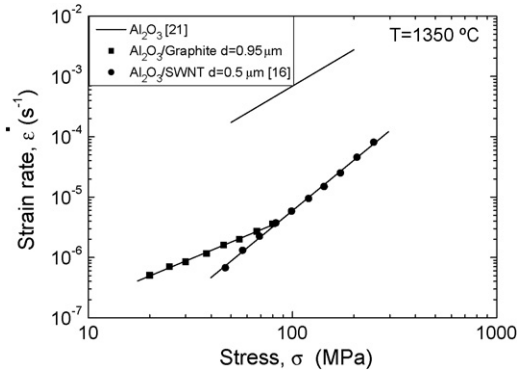

Fig. 5. Steady-state creep data for Al_2O_3/graphite composite at 1350 °C. For comparison, 1350 °C data from the literature for pure Al_2O_3 (~0.5 μm grain size)[21] and for Al_2O_3/SWNTs (~0.5 μm grain size)[16] are included.

Table 1
Al_2O_3 grain size in the Al_2O_3/graphite composite before and after creep deformation.

Grain size (μm)			
As-received	Deformed		
	1250 °C	1300 °C	1350 °C
0.95 ± 0.07	0.92 ± 0.08	0.96 ± 0.08	1.09 ± 0.09

indication of a different creep mechanism in these two composites. This difference in behaviour compared with the present composites is not surprising in view of the different microstructures.

The Al_2O_3 grain size data for before and after creep deformation are tabulated in Table 1, which shows no appreciable difference in the grain sizes. Also, dislocations activity is not observed and we do not observe grain-shape change in the Al_2O_3 grains, at least in the range of the deformation attained in our experiments.

4. Discussion

The data in Figs. 3 and 4 are analyzed using the following equation[24]:

$$\dot{\varepsilon} = A\left(\frac{\sigma}{G}\right)^n D_0^{\text{eff}} \exp\left[\frac{-Q}{RT}\right], \quad (1)$$

where A is a constant that includes the grain size dependence, G is the shear modulus, n is the stress coefficient, D_0^{eff} is the pre-exponential term of an effective diffusion coefficient, R is the gas constant, and Q is the activation energy. The values of n from the straight line fits in Fig. 3 are found to be 1.0, 1.1, and 1.4 for 1250, 1300, and 1350 °C, respectively. The value of Q is determined to be 600 ± 40 kJ/mol at 100 MPa (by extrapolation and intrapolation of data in Fig. 4). In comparison, for the pure Al_2O_3 $n \sim 1.7$ and $Q \sim 460$ kJ/mol,[23] and for the Al_2O_3/SWNTs composite $n \sim 2.6$ and $Q \sim 660$ kJ/mol.[18]

Since graphite is essentially rigid at temperatures as high as 2000 °C,[25] it is unlikely that the graphite particles are contributing to the creep deformation of the Al_2O_3/graphite composite.

Values of n ranging from 1 to 1.4 and $Q = 600 \pm 40$ kJ/mol indicates diffusional flow as deformation mechanism of the Al_2O_3,[26] with either Nabarro–Herring[27,28] or Coble[29] creep accommodated by lattice or grain-boundary diffusion, respectively.

Coble creep equation for the Al_2O_3/graphite composite can be written as follows[29]:

$$\dot{\varepsilon}_{\text{Coble}} = (1 - f)33.4\frac{\delta D_{\text{gb}} G}{kT}\left(\frac{b}{d}\right)^3\left(\frac{\sigma}{G}\right), \quad (2)$$

where D_{gb} is the grain-boundary diffusion coefficient of the rate controlling species, b is the Burgers vector, δ is the effective width of the grain boundary, and f, the volume fraction of the rigid graphite inclusions is equal to 0.1 with a discontinuous inclusions distribution. That is a small factor based on a simple rule of mixtures argument to compensate for the presence of the

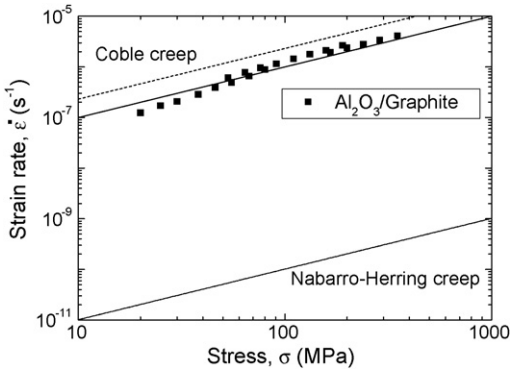

Fig. 6. Plots of the Coble and Nabarro–Herring creep models for Al_2O_3, compared to creep data for Al_2O_3/graphite composite from Fig. 3 (1300 °C).

graphite, and has only a small effect on the comparisons made in the paper. Similarly, Nabarro–Herring creep equation can be written as follows[27,28]:

$$\dot{\varepsilon}_{\mathrm{N-H}} = (1-f)9.3\frac{D_{\mathrm{l}}Gb}{kT}\left(\frac{b}{d}\right)^2\left(\frac{\sigma}{G}\right), \quad (3)$$

where D_{l} is the lattice diffusion coefficient of the rate controlling species.

Using values of $G = 150$ GPa, $b = 0.475$ nm,[30] $d = 1$ μm, $D_{\mathrm{l}} = 6.8 \times 10^{-4}$ [m^2/s] exp(−588 [kJ/mol]/RT) (lattice diffusivity of O^{2-}[29]), and $\delta D_{\mathrm{gb}} = 8.4 \times 10^{-6}$ [m^3/s] exp(−627 (kJ/mol)/RT) (grain-boundary diffusivity of O[13,31]), steady-state strain rates $\dot{\varepsilon}_{\mathrm{Coble}}$ and $\dot{\varepsilon}_{\mathrm{N-H}}$ at 1300 °C are plotted against σ in Fig. 6. These values of the diffusion coefficients are reported by Heuer[31] to be the most reliable and useful. Comparing the experimental data and the calculations in Fig. 6, it is apparent that Coble creep of the Al_2O_3 matrix controls the overall creep of the Al_2O_3/graphite composite.

5. Conclusions

The mechanical behaviour of Al_2O_3/graphite composite has been investigated. The graphite particles are found to inhibit grain-boundary sliding of Al_2O_3 grains. Therefore, the composite is restricted to deform by a diffusional mechanism. A comparison of the data with Nabarro–Herring and Coble models suggests that Coble is the mechanism controlling the plasticity of these composites.

Acknowledgements

The authors acknowledge the financial support from the Spanish "Ministerio de Ciencia e Innovación" through grant no. MAT2006-10249-C02-02. Part of this work was performed at the National Center for Electron Microscopy, Lawrence Berkeley National Laboratory, and was supported by the Office of Science, Office of Basic Energy Sciences, of the U.S. Department of Energy under Contract No. DE-AC02-05CH11231. Special thanks to Dr. V. Radmilovic and Dr. Z. Lee for further microscope training and support.

References

1. Cannon, R. M. and Coble, R. L., In *Deformation Ceramic Materials*, ed. R. L. Bradt and R. E. Tressler. Plenum Press, New York, 1975, p. 61.
2. Chokshi, A. H. and Porter, J. R., High-temperature mechanical-properties of single-phase alumina. *J. Mater. Sci.*, 1986, **21**, 705–710.
3. Ruano, O. A., Wadsworth, J. and Sherby, O. D., Deformation of fine-grained alumina by grain boundary sliding accommodated by slip. *Acta Mater.*, 2003, **51**, 3617–3634.
4. Yoshizawa, Y. and Sakuma, T., Improvement of tensile ductility in high-purity alumina due to magnesia addition. *Acta Metall. Mater.*, 1992, **40**, 2943–2950.
5. Xue, L. A. and Chen, I. W., Superplastic alumina at temperatures below 1300 °C using charge-compensating dopants. *J. Am. Ceram. Soc.*, 1996, **79**, 233–238.
6. Davies, T. J., Ogwu, A. A., Ridley, N. and Wang, Z. C., Superplasticity in ceramic materials. 1. The observation of a "superplastic partition" in ceramics. *Acta Mater.*, 1996, **44**, 2373–2382.
7. Takigawa, Y., Yoshizawa, Y. and Sakuma, T., Superplasticity in Al_2O_3–20 vol% spinel ($MgO{\cdot}1.5Al_2O_3$) ceramics. *Ceram. Int.*, 1998, **24**, 61–66.
8. Nakano, K., Suzuki, T. S., Hiraga, K. and Sakka, Y., Superplastic tensile ductility enhanced by grain size refinement in a zirconia-dispersed alumina. *Scripta Mater.*, 1997, **38**, 33–38.
9. Kim, B. N., Hiraga, K., Morita, K. and Sakka, Y., Superplasticity in alumina enhanced by co-dispersion of 10% zirconia and 10% spinel particles. *Acta Mater.*, 2001, **49**, 887–895.
10. Cho, J., Wang, C. M., Chan, H. M., Rickman, J. M. and Harmer, M. P., Role of segregating dopants on the improved creep resistance of aluminum oxide. *Acta Mater.*, 1999, **47**, 4197–41207.
11. Li, Y., Wang, C., Chan, H. M., Rickman, J. M. and Harmer, M. P., Codoping of alumina to enhance creep resistance. *J. Am. Ceram. Soc.*, 1999, **82**, 1497–1504.
12. Cho, J., Wang, C., Chan, H. M., Rickman, J. M. and Harmer, M. P., Role of segregating dopants on the improved creep resistance of aluminum oxide. *Acta Mater.*, 1999, **47**, 4197–4207.
13. Nakagawa, T., Sakaguchi, I., Shibata, N., Matsunaga, K., Mizoguchi, T., Yamamoto, T., Haneda, H. and Ikuhara, Y., Yttrium doping effect on oxygen grain boundary diffusion in alpha-Al_2O_3. *Acta Mater.*, 2007, **55**, 6627–6633.
14. Mimurada, J., Nakano, M., Sasaki, K., Ikuhara, Y. and Sakuma, T., Effect of cation doping on the superplastic flow in yttria-stabilized tetragonal, zirconia polycrystals. *J. Am. Ceram. Soc.*, 2001, **88**, 1817–1821.
15. Nakatani, K., Nagayama, H., Yoshida, H., Yamamoto, T. and Sakuma, T., The effect of grain boundary segregation on superplastic behavior in cation-doped 3Y-TZP. *Scripta Mater.*, 2003, **49**, 791–795.
16. Wang, X., Padture, N. P. and Tanaka, H., Contact-damage-resistant ceramic/single-wall carbon nanotubes and ceramic/graphite composites. *Nat. Mater.*, 2004, **3**, 539–544.
17. Poyato, R., Vasiliev, A. L., Padture, N. P., Tanaka, H. and Nishimura, T., Aqueous colloidal processing of single-wall carbon nanotubes and their composites with ceramics. *Nanotechnology*, 2006, **17**, 1770–1777.
18. Zapata-Solvas, E., Poyato, R., Gómez-García, D., Domínguez-Rodríguez, A., Radmilovic, V. and Padture, N. P., Creep-resistant composites of alumina and single-wall carbon nanotubes. *App. Phys. Lett.*, 2008, **92**, 111912.
19. Cho, J., Boccaccini, A. R. and Shaffer, M. S. P., Ceramic matrix composites containing carbon nanotubes. *J. Mat. Sci.*, 2009, **44**, 1934–1951.
20. Vasiliev, A. L., Poyato, R. and Padture, N. P., Single-wall carbon nanotubes at ceramic grain boundaries. *Scripta Mater.*, 2007, **56**, 461–463.
21. Padture, N. P., Multifunctional composites of ceramics and single-walled carbon nanotubes. *Adv. Mater.*, 2009, **21**, 1767–1770.
22. Gervais, H., Pellissier, B. and Castaing, J., Creep machine for high-temperature compression tests of ceramics. *Rev. Int. Htes. Temp. Refract.*, 1978, **15**, 43–47.
23. Xue, L. A. and Chen, I. W., Deformation and grain-growth of low-temperature-sintered high-purity alumina. *J. Am. Ceram. Soc.*, 1990, **73**, 3518–3521.

24. Poirier, J. P., *Creep of Crystals*. Cambridge University Press, Cambridge, 1985.
25. Richerson, D. W., *Modern Ceramic Engineering*. Marcel Dekker, New York, 1992.
26. Chokshi, A. H., Diffusion creep in oxide ceramics. *J. Eur. Ceram. Soc.*, 2002, **22**, 2469–2478.
27. Nabarro, F. R. N., *Report on Conf. on the Strength of Solids*. Physical Society, London, 1948, p. 75.
28. Herring, C., Diffusional viscosity of a polycrystalline solid. *J. Appl. Phys.*, 1950, **21**, 437–445.
29. Coble, R. L., A model for boundary diffusion controlled creep in polycrystalline materials. *J. Appl. Phys.*, 1963, **34**, 1679–1682.
30. Heuer, A. H., Lagerlof, K. P. D. and Castaing, J., Slip and twinning dislocations in sapphire (α-Al_2O_3). *Phil. Mag. A*, 1998, **78**, 747–763.
31. Heuer, A. H., Oxygen and aluminum diffusion in α-Al_2O_3: how much do we really understand? *J. Eur. Ceram. Soc.*, 2008, **28**, 1495–1507.